LA-UR-95-1756

TOMSK-7 RADIOCHEMICAL FACILITY EXPLOSION: CHEMICAL VESSEL BURST FAILURE ANALYSIS

Work Performed for the US Department of Energy
by Los Alamos National Laboratory
Los Alamos, NM 87545

by

E. A. Rodriguez
R. F. Davidson

Engineering & Safety Analysis Group
Technology & Safety Assessment Division

Report No.

LA-UR-95-1756

LOS ALAMOS NATIONAL LABORATORY

LA-UR-95-1756

TOMSK-7 RADIOCHEMICAL FACILITY EXPLOSION: CHEMICAL VESSEL BURST FAILURE ANALYSIS

by

E. A. Rodriguez and R. F. Davidson
Los Alamos National Laboratory

ABSTRACT

This paper develops two hypothetical failure models of the chemical vessel during the explosion at the Tomsk-7 Chemical Facility in Tomsk, Russia, and determines the burst pressure required to cause failure of the pressure vessel and the observed damage to the facility. The two failure models used in assessing the maximum pressure attained to fail the vessel and pressurize the canyon compartment are based on (1) a ductile plastic failure model and (2) a fracture mechanics evaluation. The results presented are consistent with independent analysis performed by the Russian scientists and engineers at the Tomsk-7 facility and MINATOM in Moscow. The paper shows that the maximum pressure attained before rupture was ~30 atm. These results correlate well with the subsequent canyon compartment pressurization that ejected the reinforced concrete shield plug.

INTRODUCTION

On April 6, 1993, at the radiochemical fuel reprocessing plant of the Siberian Chemical Combine in Tomsk-7, Russia, an explosion occurred that was caused by a runaway exothermic chemical reaction of a process vessel containing a concentrated solution of uranyl nitrate, nitric acid, plutonium nitrate, an uncertain amount of organics, and fission products. The explosion caused extensive structural damage to the facility and contaminated ~123 square miles with plutonium and uranium.

A United States (US)/Department of Energy (DOE) delegation of scientists and engineers, chartered by DP-35 (Office of Special Projects), visited the site and documented its findings.[1] Based on observations by the Russians and limited data provided to the US/DOE delegation of investigators, a series of preliminary analytical evaluations[2] were conducted by Los Alamos National Laboratory (LANL) in an effort to explain the causes and events. This paper extends the preliminary work performed by LANL and deals primarily with the determination of the internal pressure required to burst the process vessel and the canyon compartment pressurization that subsequently ejected the canyon shield plug into the upper gallery of the facility.

The explosion at the Tomsk-7 facility was attributed primarily to operator error; however, other factors were involved, including a lack of venting within the chemical vessel that caused the runaway reaction and subsequent breach of the pressure boundary. The loss of pressure relief was evident 10 min before the actual bursting of the pressure vessel, as described by the operators. A sketch of the chemical vessel, provided by the Tomsk-7 scientists, is depicted in Fig. 1. Control room personnel observed a system pressure increase to 0.15 atm at 12:45 p.m.

Ten minutes later, at 12:55 p.m., the pressure had increased to between 4 and 5 atm, at which point the pressure gauge registered its maximum reading. Three minutes later, at 12:58 p.m., the explosion occurred. Figure 2, also provided by the Russian scientists, shows a sketch of the failed pressure vessel, with a major longitudinal tear evident along the vessel.

The initial task was to determine the maximum amount of energy required to cause the observed structural damage to the pressure vessel and the facility. However, limited information regarding details of the vessel geometry and canyon dimensions, as well as structural details of the facility, made the evaluation speculatory at best. Nevertheless, information regarding the contents of the tank and overall volume of the canyon was supplied by the Russians that confirmed the conclusions reached by LANL.

EVALUATION

The breached condition of the vessel, as shown in Fig. 2, is evident of a classic catastrophic failure caused by longitudinal tearing of the vessel wall, presumably and most likely at a seam weld (although this has not been verified).

Several secondary tears are evident along the longitudinal opening, which is indicative of ductile tearing that is common to stainless steels. Furthermore, the chemical vessel had been in operation for a long period of time, where potential material degradation mechanisms may have taken effect. Combined with this assumption is the uncertainty with fabrication techniques, welding methods, material properties, residual stresses, and nondestructive testing (NDT).

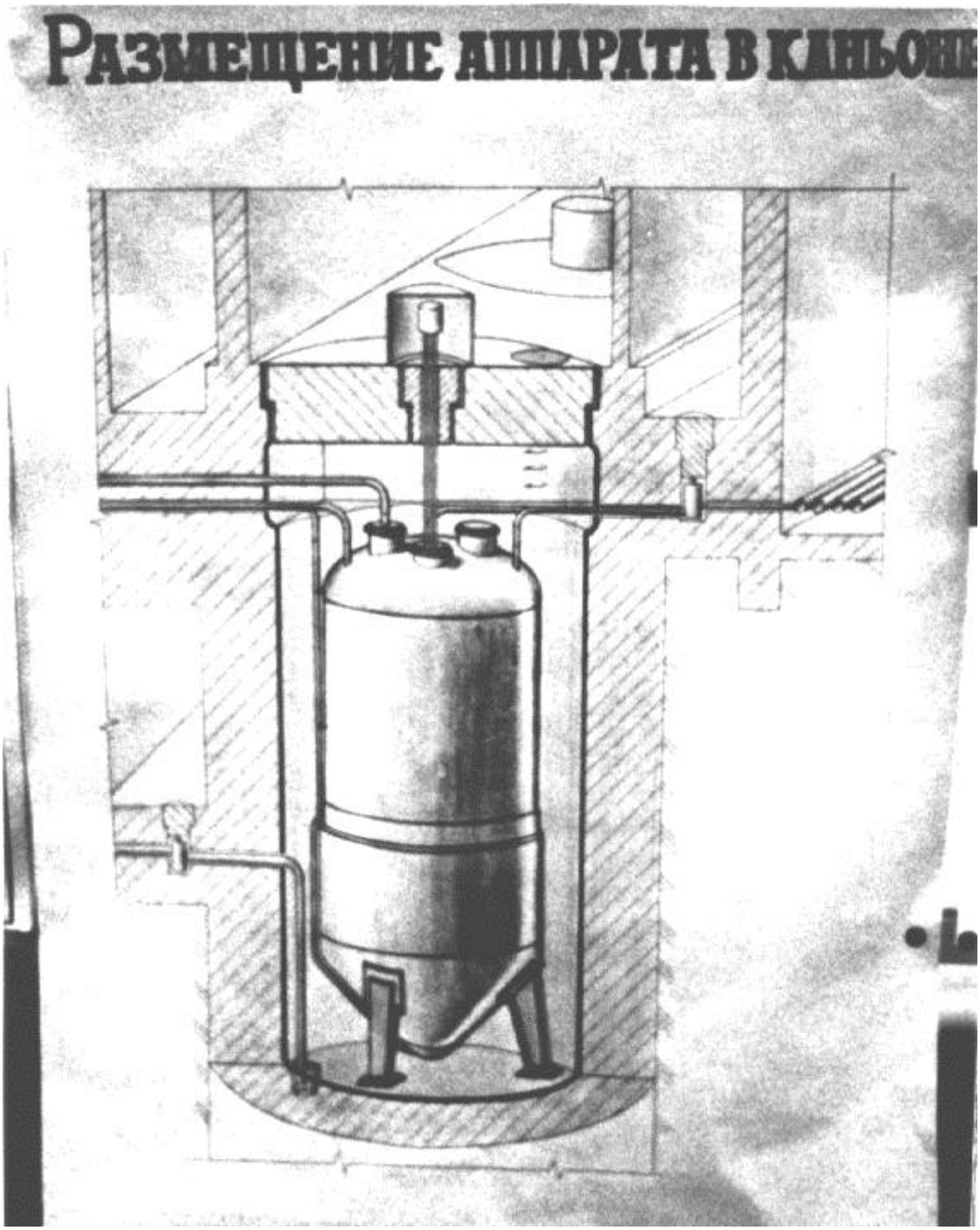

Fig. 1. Chemical vessel.

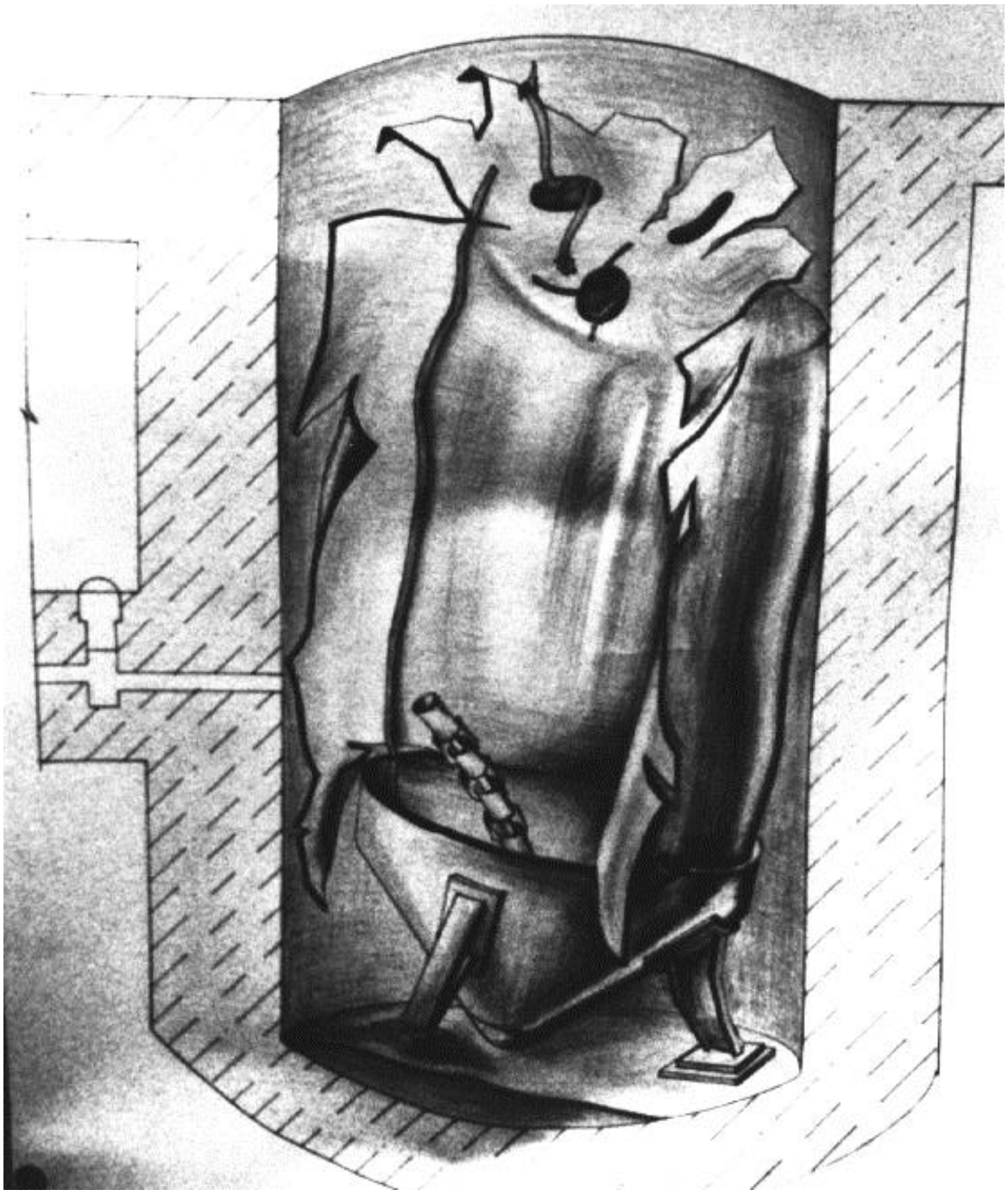

Fig. 2. Ruptured chemical vessel.

This portion of the LANL analysis effort in this report focuses on two typical failure mechanisms for pressure vessel bursting. The following topics will be addressed:

- material properties,
- vessel dimensions,
- design conditions,
- failure mechanisms
  - failure based on ductile plasticity
  - failure based on linear-elastic-fracture mechanics (LEFM), and
- maximum canyon compartment pressure.

Figure 3 shows a peak pressure of 30 atm; however, no recorded evidence exists to support this assumption. Therefore, an assumed pressure-rise function based on the observed gauge pressures at 0.15 and 5 atm (when the gauge failed) and peaking at 30 atm is:

$$P = 9.87x10^{-16}\left(t^{11.43}\right) \quad . \tag{1}$$

MATERIAL PROPERTIES

The Russian stainless steels are considered comparable in chemical composition and mechanical properties to the US specifications, with the exception of several specific Russian stainless steels that are covered in their State Standard (GOCT). However, some Russian stainless steels typically have a higher carbon content than those given in the US specifications. While no actual data has been received relative to the vessel material, the Russian stainless steels are believed to be of a low grade. In this analysis, we shall use US specifications for 304 Stainless Steel (SS), which is assumed to be similar to the Russian stainless steel.

304-SS—Comparable to the American Society for Testing and Materials (ASTM) specification for 304-SS, Gr. 70 and Gr. 80 (see Table 1). For analysis purposes, Gr. 70 steel will be assumed.[3]

The 304-SS material yield and ultimate tensile strength temperature dependence for Gr. 70 is shown in Fig. 4.

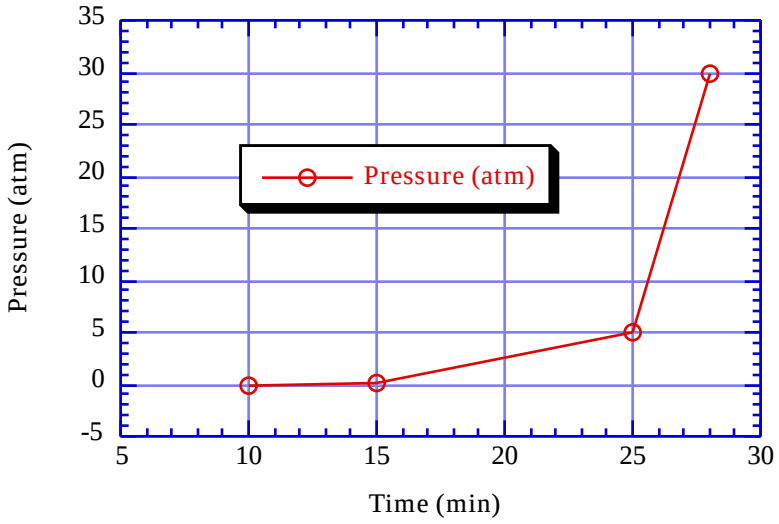

Fig. 3. Assumed pressure rise in the chemical vessel.

TABLE 1
STAINLESS-STEEL MATERIAL PROPERTIES

Material Grade	Temperature [°F (°C)]	Yield Strength [ksi (kg/cm^2)]	Ultimate Strength [ksi (kg/cm^2)]
Gr. 70	100 (~40)	25.0 (1760)	70.0 (4920)
	275 (135)	20.0 (1400)	62.0 (4360)
Gr. 80	100 (~40)	35.0 (1760)	80.0 (4570)
	275 (135)	26.0 (1830)	77.0 (5410)

The strain-hardening exponent for 304-SS is reported to be in the range of:

$$n = 0.585 \text{ to } 0.724 \quad .$$

For design purposes, typical values of strain hardening normally are given as >0.3; however, the range of actual test data[4,5] are as shown above. The following analysis will use the lower-bound value of the strain-hardening exponent.

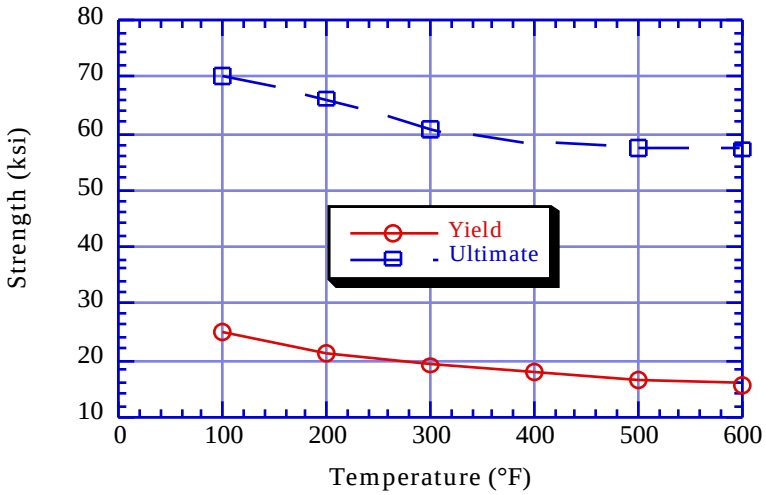

Fig. 4. Strength-temperature characteristic for 304-SS, Gr. 70.

VESSEL DESCRIPTION

The chemical vessel is used for plutonium-uranium extraction (PUREX) processing and is situated in a canyon-type facility similar to those used in US facilities. At the time of the explosion, the vessel contained ~23,500 L of uranyl nitrate, as well as 1500 L of nitric acid and ~500 L of a floating organic layer. The vessel dimensions are shown in Fig. 5. (These are actual dimensions from Russian fabrication drawings.)

The tank wall (t_w) thickness may vary throughout the vessel length; however, the majority of the vessel plate material, and in particular where the fracture took place, was manufactured from 14-mm-thick steel.

t_w = 14 to 18 mm (0.551 to 0.709 in.) .

The main portion of the shell where rupture failure was initiated is 14 mm thick.

DESIGN CONDITIONS

It is assumed that the Russian design criteria for pressure vessels is similar to the US standards, as ascribed by the American Society of Mechanical Engineers (ASME) Boiler & Pressure Vessel Code.[3] As such, it is important to first determine the pressure capacity of the original design to fully assess the potential capacity at failure.

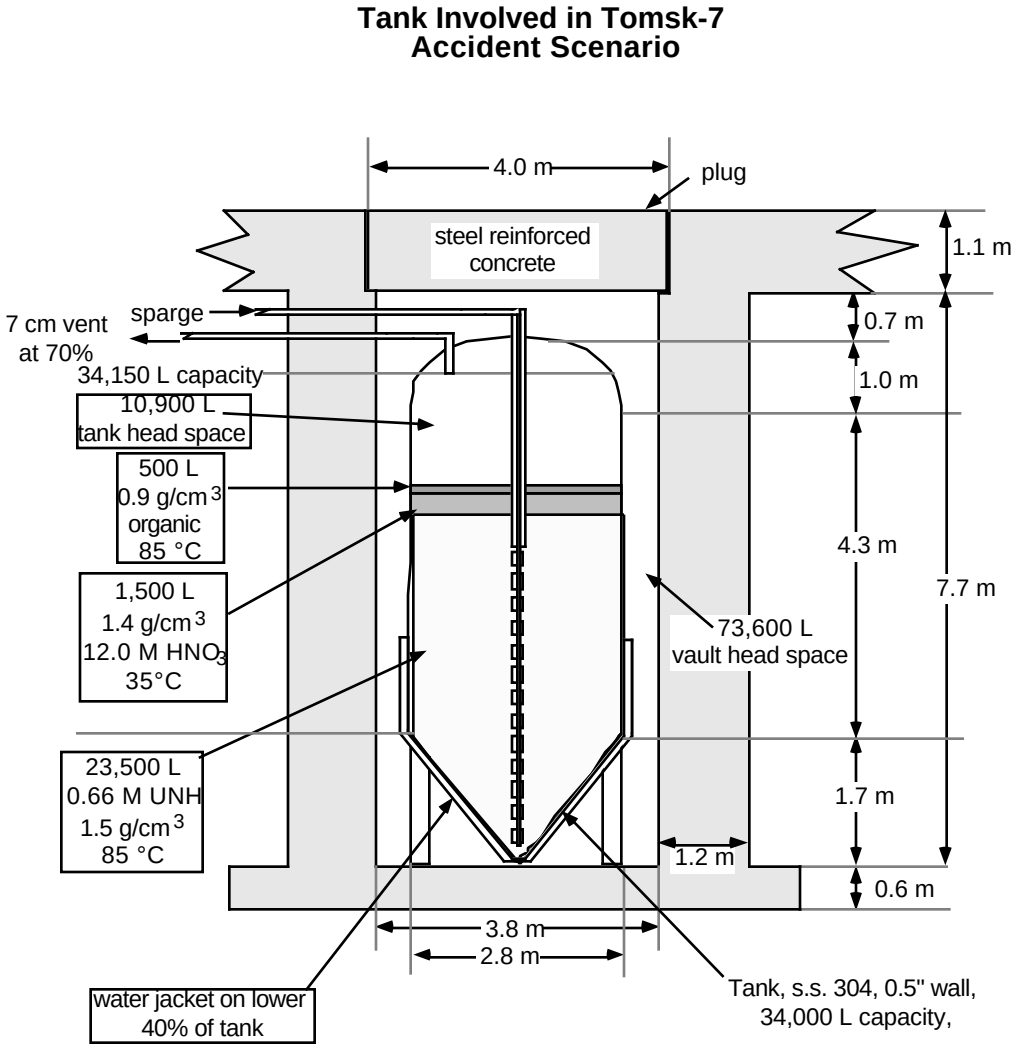

Fig. 5. Chemical vessel dimensions.

- The original design of the vessel

  - assumes that design criteria used for vessel is comparable to the ASME Code rules for design;
  - applies an allowable stress equivalent to the lower of 2/3 of the material yield strength or 1/3 of the ultimate tensile strength for the design membrane stress intensity; and
  - bases the maximum design pressure on the ASME Code, Section III, Subsection NB, maximum membrane stress intensity.

The maximum membrane stress intensity is defined as the difference of the two principal stresses. In a cylindrical vessel, the maximum stress intensity is derived in the circumferential and radial direction:

$$\sigma_p = \sigma_h - \sigma_r \tag{1}$$

$$\sigma_h = \frac{P_d R}{t} \qquad \sigma_r = -\frac{P_d}{2} \quad , \tag{2}$$

where

σ_p = maximum principal stress (ksi),
σ_h = hoop stress in vessel (ksi),
σ_r = radial stress (through-thickness) (ksi),
P_d = design pressure (at 135°C), and
R = radius of vessel (in.).

The design pressure was calculated to be in the range of:

P_d = 12 to 16 atm.

Therefore, based on the range of minimum and maximum yield strengths considering metal temperatures of 275°F (135°C), the chemical separation vessel (potentially) was designed to withstand internal pressures of 12 to 16 atm. This implies that, if we consider a flawless condition to the operating vessel, the internal pressure necessary to develop a membrane stress equivalent to the material yield strength is:

P_b = 18 to 24 atm.

Therefore, allowing for the strain-hardening nature of stainless steels, it is assumed that the burst pressure would be ~1.5 times the yield (see Table 2). In which case, given the ductile nature of the material, the burst pressure would be in the range of:

P_b = 30 atm.

FAILURE MECHANISMS

Ductile Plastic Failure

Failure of ductile materials is characterized by large strains well into the plastic regime noted to cause tearing before catastrophic failure. Bursting is a plastic instability that is recognized to increase the volume of the vessel while

TABLE 2
COMPARISON OF DESIGN AND BURST PRESSURES

Design Pressure (atm)	Yield Pressure (atm)	Burst Pressure (atm)
12	18	27
16	24	36

decreasing the pressure. Langer[3] and Cooper[4] each derived expressions for the theoretical burst pressure of cylindrical vessels for ductile materials based on strain-hardening relationships similar to the inverse form of the Ramburg-Osgood equation:[6]

$$\sigma_t = C_1 \varepsilon^{n} + C_2 \quad , \tag{3}$$

where

σ_t = true stress (ksi),
C_1 = strength coefficient,
C_2 = constant (usually the yield strength),
ε = true strain (in./in.), and
n = strain hardening exponent.

For typical 304-SS with a yield strength in the 35-ksi range, the following values have been derived and documented[3] for the strain-hardening relationship (see Fig. 6):

C_1 = 171000 psi,
C_2 = 36800 psi, and
n = 0.585 (min).

$$\sigma_t = \left(1.71x10^5\right)\varepsilon^{0.585} + 36800 \quad . \tag{4}$$

Correcting the above equation to conform to a 25-ksi yield-strength material, we obtain:

$$\sigma_t = \left(1.71x10^5\right)\varepsilon^{0.585} + 25000 \quad . \tag{5}$$

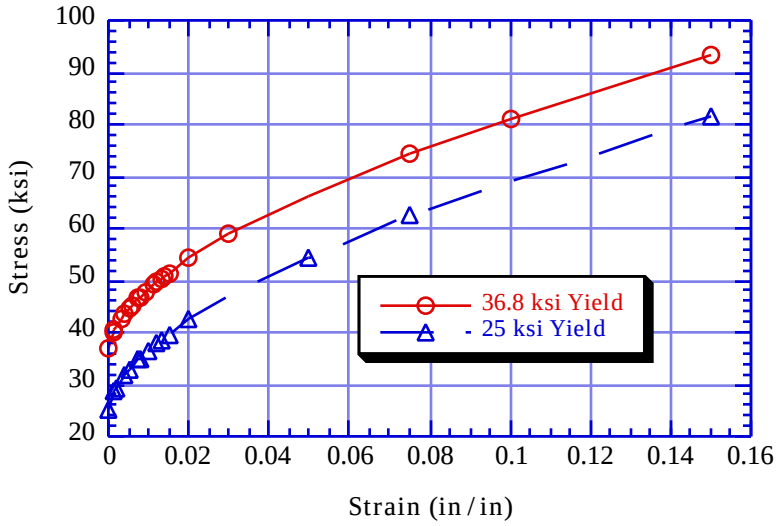

Fig. 6. True stress-strain relationship for typical 304-SSs.

For thin-walled cylindrical vessels, both forms obtain similar results and are summarized below:

$$P_b = 2.31[0.577]^n\left(\frac{t_w}{D_i}\right)S_u \qquad \text{(Langer)},^4 \tag{6}$$

and

$$P_b = 2[3]^{-\left(\frac{n+1}{2}\right)}\left(\frac{t_o}{R_o}\right)S_u \qquad \text{(Cooper)}.^5 \tag{7}$$

Using the expression by Langer for the burst pressure:

$$P_b = 2.31[0.577]^n\left(\frac{t_w}{D_i}\right)S_u \quad ,$$

where

P_b = burst pressure (ksi),
n = strain-hardening exponent,
t_w = shell wall thickness (in.),
t_o = initial shell-wall thickness (in.),

D_i = inside diameter (in.),
R_o = initial mean radius (in.), and
S_u = ultimate tensile strength (ksi).

The failure surface has not been examined metallographically; therefore, questions remain as to the state of the vessel under operation. It is believed that failure was along a seam weld, based on the apparent fracture surface. The effect of welding, residual stresses, and strain concentrations has not been addressed. However, Royer and Rolfe[7] concluded that nominal or moderate strain concentrations generally do not lower the burst pressure.

Therefore, based on the possible variation of the strain-hardening exponent and such relevant material properties as tensile strength and vessel geometry, the most probable burst pressure would be:

P_b **= 33 atm**.

Brittle Fracture

Although stainless steels are considered ductile materials and generally do not behave in a brittle manner, an approximation to failure by brittle fracture was conducted using LEFM. Stainless steels, as with all ductile materials, have a tendency to tear plastically instead of fracturing in a brittle manner.

Therefore, an Elastic-Plastic Fracture Mechanics (EPFM) model would be much more accurate in the determining the failure pressure assuming embedded flaws. Details of the pre-failure surface geometry must be known to develop a realistic fracture solution adequately. In the future, the possibility of conducting evaluations of the failure surface through metallographic and fractographic examination may be hampered by decontamination efforts or the possibility that the vessel has been scrapped.

Nevertheless, for purposes of evaluating the maximum possible energy release, an LEFM model for two possible types of flaws are evaluated. The first is assumed to be a longitudinal through-wall flaw in a large plate. The large plate assumption seems valid because the radius-to-thickness ratio of the vessel is ~100, implying that curvature effects may be neglected. The second is a semi-elliptical surface flaw that is part through-wall.

The stress intensity factor for the flaw is given by:

$$K_{IC} = C\sigma\sqrt{\pi a} \quad , \tag{8}$$

where

K_I = stress intensity factor for flaws $ksi\sqrt{in}$,
C = geometric constant,
σ = circumferential stress in cylinder (ksi), and
a = flaw half-length (in.).

1. Through-Wall Flaw (see Fig. 7):

$$C = \left[\frac{2b}{\pi a}\tan\left(\frac{\pi a}{2b}\right)\right]^{1/2} \tag{9}$$

where

b = cylinder length (in.).

For this geometry, the constant C approximates the value of a flaw in an infinitely long plate. While the constant is dependent on the flaw's half-length to plate width, the constant approximates unity for realistic flaw sizes. That is, the constant C = 1.0.

2. Semi-Elliptical Surface Flaw (see Fig. 8):

$$K_I = 1.12\sigma\sqrt{\frac{\pi a}{Q}}M_k \quad , \tag{10}$$

where

Q = flaw shape factor, also dependent on yield strength; and
M_k = back-face correction factor.

If we assume that a circular-type flaw is embedded halfway through the vessel wall, the maximum stress intensity factor is:

$$K_I = 0.65\sigma\sqrt{\pi a} \quad , \tag{11}$$

Q = 2.4, and
M_k = 1.0.

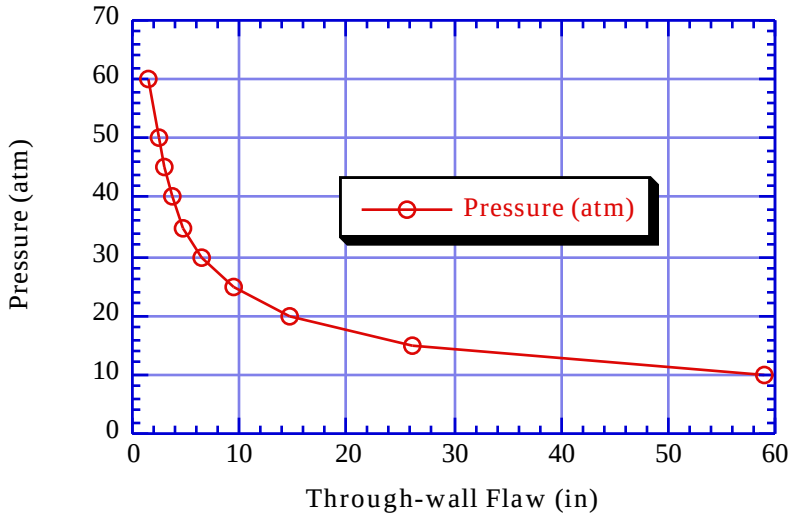

Fig. 7. Critical flaw size at burst pressure for through-wall flaw.

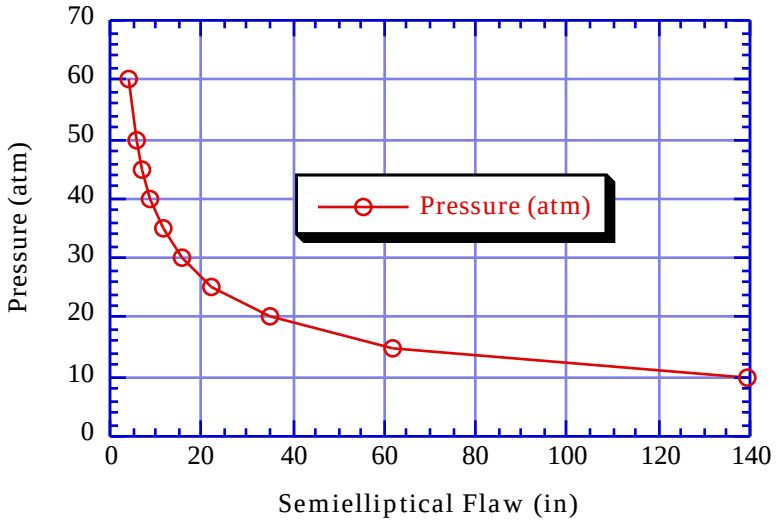

Fig. 8. Critical flaw size at burst pressure for semi-elliptical flaw.

The stress intensity factor K_I calculated above for a given flaw size then is compared to the upper-bound critical stress intensity factor K_{IC}, which is commonly called the plane-strain fracture toughness of the material. The fracture toughness is a material property determined from compact tension specimens in accordance with ASTM (E-399). At the onset of crack propagation,

the calculated stress intensity factor, based on the crack-driving stress, will be equal to or greater than the material's fracture toughness. That is:

$$K_I \geq K_{IC} \quad .$$

Because actual values of fracture toughness K_{IC} are not available for the vessel material, a good estimate can be obtained by using approximate values of the elastic-plastic critical energy release, J_{IC}, for common 304-SS and typical published[8,9] values of K_{IC}.

Typical values for 304-SS (within the elastic region) are shown in Table 3. The elastic-plastic energy release is related to the plane-strain fracture toughness by:

$$J_{IC} = \frac{K_{IC}^2}{E} \quad , \tag{12}$$

where

E = modulus of elasticity (psi), and

$$K_{IC} = \sqrt{J_{IC} E} \quad . \tag{13}$$

The corresponding critical stress-intensity K_{IC} values are shown in Table 3.

TABLE 3
ELASTIC-PLASTIC FRACTURE TOUGHNESS AND PLANE-STRAIN FRACTURE TOUGHNESS

J_{IC} $\left(in - lb / in^2\right)$	K_{IC} $\left(ksi\sqrt{in}\right)$	Yield Strength (ksi)	Temperature (°F)
975 (Ref. 8)	165	25	100
1150 (Ref. 8)	180	25	100
1500 (Ref. 7)	200	25	316
4000 (Ref. 7)	335	45	100

Using the median K_{IC} value of $200 ksi\sqrt{in}$ from Table 3 and solving for the maximum hoop membrane stress as a function of flaw size:

$$\sigma = \frac{PR}{t} \quad .$$

The through-wall flaw stress intensity is:

$$K_{IC} = \left(\frac{PR}{t}\right)\sqrt{\pi a} \quad , \tag{14}$$

or

$$a = \frac{1}{\pi}\left[\frac{K_{IC}}{\left(\frac{t}{R}\right)P}\right]^2 \quad . \tag{15}$$

The semi-elliptical surface flaw stress intensity is:

$$K_I = 0.65\left(\frac{PR}{t}\right)\sqrt{\pi a} \quad , \tag{16}$$

or

$$a = \frac{1}{\pi}\left[\frac{K_{IC}}{\left(\frac{t}{R}\right)0.65P}\right]^2 \quad . \tag{17}$$

Table 4 itemizes the results of solving for the flaw sizes of both the through-wall and semi-elliptical cases as a function of the maximum pressure for brittle fracture. Table 4 and Fig. 9 show that for credible burst pressures, the flaw sizes associated with these pressures are ~6 to 10 in. in length.

TABLE 4
CRITICAL FLAW SIZE BASED ON BURST PRESSURE

	Flaw Size (in.)	
Pressure (atm)	**Through-Wall Flaw**	**Semi-Elliptical Surface Flaw**
10	58.9	139.5
15	26.2	62.0
20	14.7	34.9
25	9.4	22.3
30	6.5	15.5
35	4.8	11.4
40	3.7	8.7
45	2.9	6.9
50	2.4	5.6
60	1.6	3.9

We neglect burst pressures >40 atm because these are beyond the practical limits of the material's ductility; we also neglect burst pressures <20 atm because these are associated with very large initial flaws. Furthermore, the equivalent length through-wall flaw, as compared to the semi-elliptical surface flaw, is associated with a lower pressure to cause brittle fracture of the vessel. The pressure to cause a brittle fracture is taken conservatively to be between 25 and 35 atm for three reasons.

- First, the design capacity of the vessel is ~12 to 18 atm, while maintaining membrane stresses well below the yield strength. Consequently, the yield capacity was shown to be ~18 to 24 atm.

- Second, as mentioned above, it is not credible that the vessel could withstand pressures >35 to 40 atm, based purely on an elasticity point of view of the material's ductility. The material would rupture above 35 to 40 atm, even if the vessel material were in a pristine state.

- Third, for pressures <20 atm, the initial flaw lengths would have to be extremely large for brittle fracture to occur. For large initial flaws to be credible, a leak-before-break scenario would have occurred,

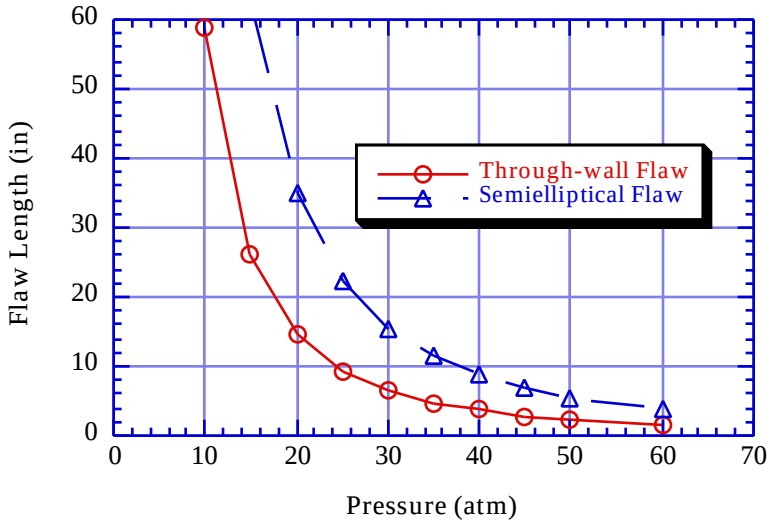

Fig. 9. Comparison of flaw sizes.

and there would not have been a catastrophic failure. In other words, given a large flaw size with a lower burst pressure, the tendency is to relieve the internal pressure by allowing leakage rather than catastrophic failure from bursting.

This again coincides with the Russian scientists' observations at Tomsk-7. It should be understood that because stainless steel is quite ductile compared to other types of steel, the assumption of using LEFM criteria is not altogether correct. EPFM may provide a better correlation of the pressure at instability for

a given credible flaw size. Nevertheless, the LEFM technique provides a very good estimate of the maximum internal pressure at fracture.

MAXIMUM PRESSURIZATION IN CANYON COMPARTMENT

The bursting of the vessel expelled steam into the canyon compartment, which filled the complete volume. The steam pressure subsequently ejected the 38-ton reinforced concrete shield plug, situated immediately above the vessel, into the upper building gallery. The shield plug later was found ~10 to 15 m from the canyon access. The canyon compartment volume is known to be ~100.5-m^3, and the approximate dimensions are as shown in Fig. 10. Parameters are given in Table 5.

Before the explosion, the canyon compartment was known to contain ~1.5 m^3 of solid material, including the vessel shell structure, auxiliary piping, and vessel supports. It is assumed that the bursting occurred at or near the saturation pressure of steam. As the pressure began to increase in the vessel, the steam could expand only to the free volume of the tank, which was noted at ~10.9 m^3. However, there was ~25.5 m^3 of combined uranyl nitrate and nitric acid liquid solution plus 0.5 m^3 of organic layer remaining in the vessel. Therefore, the free compartment volume at the time of the explosion accounting for all the material was ~73.6 m^3. The maximum compartment pressure based on a simple isentropic volumetric expansion of the steam in the tank is calculated from:

$$P_1V_1 = P_2V_2 \quad .$$

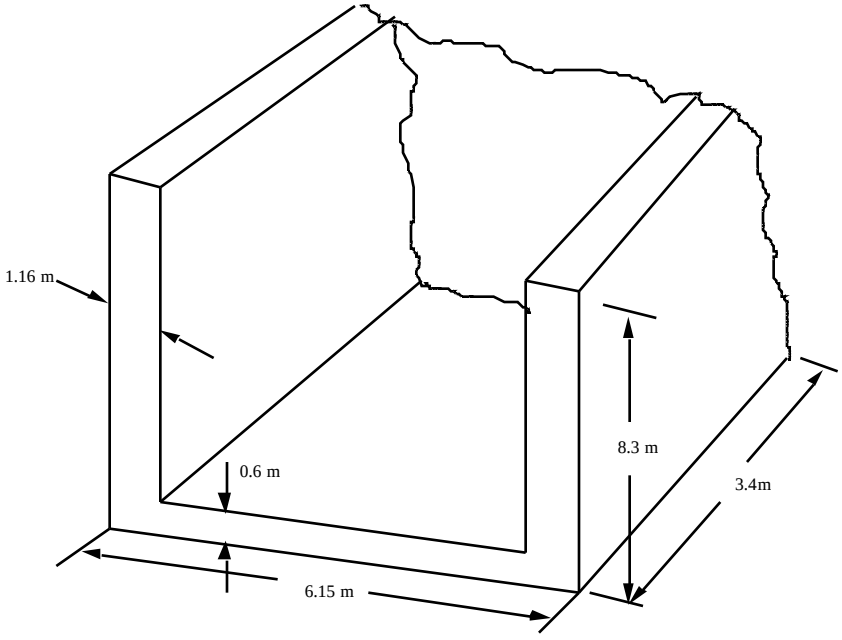

Fig. 10. Canyon compartment dimensions.

TABLE 5
CANYON COMPARTMENT PARAMETERS

Parameter	Volume (m^3)
Tank (Free Volume)	10.9
Liquid / Organics	25.5
Compartment	100.5
Metal	1.5

If a vessel burst pressure in the range of 30 to 35 atm is used, the compartment pressure is estimated to be:

P_C **= 4 - 5 atm.**

Russian scientists and engineers at Tomsk-7 also confirmed that the compartment pressurization reached ~4 to 5 atm, based on their independent failure analysis. Therefore, the vessel burst pressure is confirmed to be ~30 atm.

CONCLUSIONS

- The design operating capacity of the chemical vessel indicates maximum pressures of 12 to 16 atm at stresses well below the yield strength. At the onset of yielding, the maximum pressure is shown to be 18 to 24 atm.

- A simple ductile failure mechanism for cylindrical vessels, based on the typical stainless-steel strain-hardening exponent, predicts the burst pressure of the chemical vessel at 30 to 35 atm.

- Credible flaw sizes based on a linear-elastic fracture mechanics evaluation determined the burst pressure to be 25 to 35 atm.

- The maximum compartment pressurization based on the vessel burst pressure and volumetric expansion of steam was shown to be 4 to 5 atm.

Therefore, we conclude that the maximum pressure causing vessel failure is 30 atm. These results are in agreement with observed damage and independent analyses by the Tomsk-7 scientists and engineers.

ACKNOWLEDGMENTS

This work was performed by Los Alamos National Laboratory, which is administered by the University of California for the US Department of Energy. The US-DOE Office of Defense Programs, DP-35, provided the initial information and contacts with the Russian Federation and the Ministry of Atomic Energy (MINATOM).

REFERENCES

1. F. C. Gilbert et al, "Trip Report—Moscow and Tomsk, Russia," US Department of Energy, Office of Defense Programs trip report #DOE/DP-0120 (September 1993).

2. S. W. Eisenhawer, S. F. Agnew, R. F. Davidson, E. A. Rodriguez, and J. R. Travis, "An Interim Report on Modeling of the Tomsk-7 Accident," Los Alamos National Laboratory report LA-UR-95-1075 (March 1995).

3. American Society of Mechanical Engineers (ASME) Boiler and Pressure Vessel Code, Section VIII, Div. 2, *Pressure Vessels* (American Society of Mechanical Engineers, New York, NY, 1989).

4. B. F. Langer, "Pressure Vessel Research Council Interpretive Report of Pressure Vessel Research—Section 1: Design Considerations," Welding Research Council Bulletin # 95 (April 1964).

5. W. E. Cooper, "The Significance of the Tensile Test to Pressure Vessel Design," Welding Research Supplement (1957).

6. J. Chakrabarty, *Theory of Plasticity* (McGraw-Hill Book Company, New York, 1987).

7. C. P. Royer and S. T. Rolfe, "Effect of Strain-Hardening Exponent and Strain Concentrations on the Bursting Behavior of Pressure Vessels," Transactions of the ASME, Journal of Engineering Materials and Technology (October 1974).

8. W. H. Bamford and A. J. Bush, "Fracture Behavior of Stainless Steel," ASTM STP 668, ASTM 1979, pp. 553–557.

9. J. M. Holt, H. Mindlin, and C. Y. Ho, *Structural Alloys Handbook*, (CINDAS/Purdue University, West Lafayette, Indiana, 1992), Vol. 2.